



HAL
open science

Stratigraphic correlations between the European Project for Ice Coring in Antarctica (EPICA) Dome C and Vostok ice cores showing the relative variations of snow accumulation over the past 45 kyr

R. Udisti, S. Becagli, E. Castellano, B. Delmonte, J. Jouzel, J.R. Petit, J. Schwander, B. Stenni, E.W. Wolff

► To cite this version:

R. Udisti, S. Becagli, E. Castellano, B. Delmonte, J. Jouzel, et al.. Stratigraphic correlations between the European Project for Ice Coring in Antarctica (EPICA) Dome C and Vostok ice cores showing the relative variations of snow accumulation over the past 45 kyr. *Journal of Geophysical Research*, 2004, 109 (D8), 10.1029/2003JD004180 . hal-03109879

HAL Id: hal-03109879

<https://hal.science/hal-03109879>

Submitted on 14 Jan 2021

HAL is a multi-disciplinary open access archive for the deposit and dissemination of scientific research documents, whether they are published or not. The documents may come from teaching and research institutions in France or abroad, or from public or private research centers.

L'archive ouverte pluridisciplinaire **HAL**, est destinée au dépôt et à la diffusion de documents scientifiques de niveau recherche, publiés ou non, émanant des établissements d'enseignement et de recherche français ou étrangers, des laboratoires publics ou privés.

Stratigraphic correlations between the European Project for Ice Coring in Antarctica (EPICA) Dome C and Vostok ice cores showing the relative variations of snow accumulation over the past 45 kyr

R. Udisti,¹ S. Becagli,¹ E. Castellano,¹ B. Delmonte,^{2,3} J. Jouzel,⁴ J. R. Petit,² J. Schwander,⁵ B. Stenni,⁶ and E. W. Wolff⁷

Received 24 September 2003; revised 9 February 2004; accepted 24 February 2004; published 16 April 2004.

[1] High-resolution chemistry analysis and electrical measurements performed on two ice core records (European Project for Ice Coring in Antarctica (EPICA) Dome C and Vostok) spanning the last 45 kyr allow stratigraphic correlations by matching volcanic events. Several common events were identified along the two ice cores on the basis of acidity and sulphate spikes in snow layers. Timescales were matched through comparison with isotope (δD) profiles and using the Antarctic cold reversal (ACR) minimum, a ^{10}Be peak, and a dust spike as temporal checkpoints. Ratios of relative snow accumulation at the two sites during the Holocene, in the glacial-interglacial transition and in the last part of the glacial period, were reconstructed by finding the best fit between Dome C and Vostok depths recording the same events. After accounting for thinning of the layers as they are buried within the glacier, the Dome C-Vostok accumulation ratio, expected to be roughly constant from the conventional accumulation-temperature-isotope approach, is 1.12 for the glacial period but increases to as much as 1.44 for a large part of the Holocene. Glaciological effects, mainly related to the geographic origin of the Vostok ice along the Ridge B-Vostok axis, can account for only a minor fraction of this change. Instead, we argue that accumulation variability between the cores stems from differential changes in atmospheric circulation during these respective climatic periods at the two sites. Regional changes in atmospheric circulation are proposed with a negative anomaly in Dome C, a positive accumulation anomaly in Vostok, or a combination of both during glacial climate. Our approach may help to improve ice core dating by: (1) revealing anomalies in accumulation-rate estimation based on the classical thermodynamic method and (2) supporting the necessity to take into account contributions due to changes in atmospheric circulation processes. *INDEX TERMS*: 0325 Atmospheric Composition and Structure: Evolution of the atmosphere; 1620 Global Change: Climate dynamics (3309); 1863 Hydrology: Snow and ice (1827); 3344 Meteorology and Atmospheric Dynamics: Paleoclimatology; 9310 Information Related to Geographic Region: Antarctica; *KEYWORDS*: Antarctic ice core comparison, accumulation rate changes, glacial-Holocene atmospheric circulation changes

Citation: Udisti, R., S. Becagli, E. Castellano, B. Delmonte, J. Jouzel, J. R. Petit, J. Schwander, B. Stenni, and E. W. Wolff (2004), Stratigraphic correlations between the European Project for Ice Coring in Antarctica (EPICA) Dome C and Vostok ice cores showing the relative variations of snow accumulation over the past 45 kyr, *J. Geophys. Res.*, 109, D08101, doi:10.1029/2003JD004180.

1. Introduction

[2] The study of physical and chemical properties of ice cores drilled in the polar regions provides detailed information about past atmospheric composition and climatic variability. Paleoenvironmental information is now recovered for time periods spanning several hundreds of millennia, with a time resolution even subannual for the last millennia. Deep ice cores drilled in central Greenland and Antarctica allow a better understanding of forcing and feedback factors of global climatic changes [e.g., Dansgaard *et al.*, 1993; Legrand and Mayewski, 1997; Lorius, 2000; Petit *et al.*, 1999].

[3] A reliable comparison between chemical and physical data sets from different ice cores is essential for a correct

¹Department of Chemistry, University of Florence, Florence, Italy.

²Laboratoire de Glaciologie et Géophysique de l'Environnement du CNRS, Saint-Martin-d'Hères Cedex, France.

³Also at Department of Environmental Science, University of Milano-Bicocca, Milan, Italy.

⁴Laboratoire des Sciences du Climat et de l'Environnement, Unité Mixte de Recherche Centre Energie Atomique-CNRS, Gif-sur-Yvette, France.

⁵Physics Institute, University of Bern, Bern, Switzerland.

⁶Department of Geological, Environmental and Marine Sciences, University of Trieste, Trieste, Italy.

⁷British Antarctic Survey, Natural Environment Research Council, Cambridge, UK.

interpretation of paleoclimatic variations. The correlation between climatic and environmental proxies from nearby ice cores provides information about local to hemispheric variability [Cole-Dai *et al.*, 1997; Cole-Dai and Mosley-Thompson, 1999], giving insights on interhemispheric variability and evidence for synchronicity or lead/lags of global events [Langway *et al.*, 1995].

[4] A key issue of paleoclimatic reconstruction from ice cores is the dating of the stratigraphic sequences. For central Antarctic sites, accumulation rates are very low and wind scouring generally disturbs the snow surface with the consequence that the annual layers are poorly preserved [Schwander *et al.*, 2001; Petit *et al.*, 1982]. As no absolute dating method is available for old ice, ice core chronology is based on a glaciological model that takes into account ice dynamics, thinning of the layers as they are buried in the glacier, and variation of the accumulation rate with climate. Parameters of the model are best adjusted by matching of the ice core record to known dated events: e.g., climatic events recorded in dated marine records [e.g., Petit *et al.*, 1999], cosmic events such as the ^{10}Be event at 41 kyr BP [Schwander *et al.*, 2001], or volcanic events [Cole-Dai *et al.*, 1997; Cole-Dai and Mosley-Thompson, 1999; Udisti *et al.*, 2000]. A chronology has to be developed for each ice core since model parameters are different from site to site. As a result, age offsets always appear when comparing two paleoclimatic records from Antarctic cores. Questions arise about the choice of the most reliable chronology, or how to improve the dating, while still allowing glaciological model parameters to be realistic. For this issue, a first step is to choose a site where the ice movement is small and the glaciological model is theoretically simpler than for a site located on a flow line. In this matter, the European Project for Ice Coring in Antarctica (EPICA) selected a dome area (Dome C) to perform a deep ice core drilling that may cover almost the last million years [EPICA Dome C 2001–02 Science and Drilling Teams, 2002]. A second step for accurate comparison between different ice core records is the search for common events recorded in each ice core. This would allow synchronization and a direct comparison on a common depth scale, for which a chronology could be chosen. As an example, matching between Dome C and Vostok volcanic signatures from 1200 to 7100 years BP was used to transfer a dated Vostok ice core sequence (through a link between ^{10}Be in ice and ^{14}C) to EPICA-Dome C and set the Dome C timescale named “EDC1” [Schwander *et al.*, 2001, and references therein]. Concerning Greenland ice cores, a similar strategy was used to synchronize GISP2 and GRIP ice cores by matching electrical and chemical signatures [e.g., Southon, 2002; Taylor *et al.*, 1993]. So far, no detailed information on relative accumulation-rate changes from glacial to Holocene period are available from ice core comparisons both in Antarctica and in Greenland.

[5] In this paper, we describe the stratigraphic correlation between the EPICA Dome C ice core (EDC96), a 788 m core that covers the last 45 kyr [Schwander *et al.*, 2001], and the upper part of the Vostok ice core record by using volcanic events. Previous papers compared Vostok and EDC96 Electrical Conductivity Measurements (ECM) profiles [Wolff *et al.*, 1999] for the last 10 kyr, and sulphate and ECM volcanic signatures in the EDC96 ice core [Udisti *et al.*, 2000]. Here we extend the comparison over the last

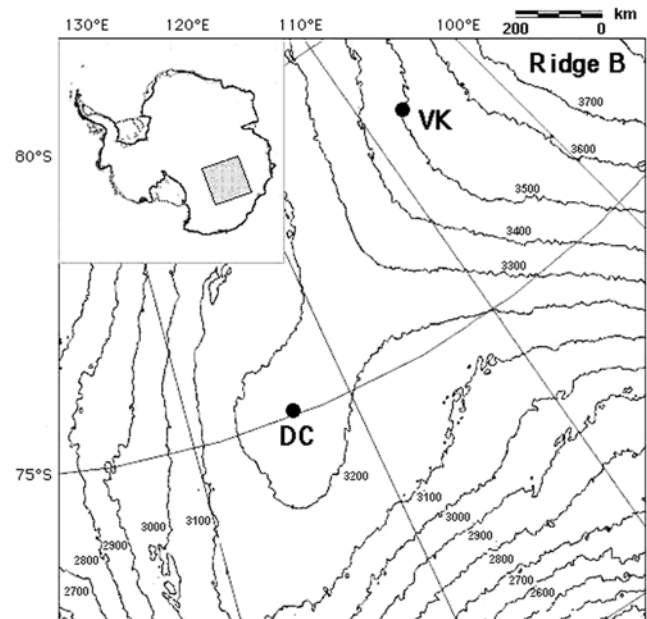


Figure 1. Map of Antarctica showing the Vostok (VK), Dome C (DC) and Ridge B locations.

45 kyr, and synchronize the two ice core depth scales independently from their dating models. Glaciological and potential climatic effects on accumulation ratio variations are discussed in order to assess the role of atmospheric circulation changes on central Antarctica snow deposition.

2. Ice Core ECM and Chemistry Processing

[6] Dome C ($75^{\circ}06'S$; $123^{\circ}21'E$; 3233 m asl, present accumulation rate: $2.7 \text{ g cm}^{-2} \text{ a}^{-1}$) and Vostok ($78^{\circ}30'S$, $106^{\circ}50'E$, 3480 m asl, present accumulation rate: $2.2 \text{ g cm}^{-2} \text{ a}^{-1}$) are located in central East Antarctica, about 600 km apart (Figure 1). Drilling of the first Dome C ice core (named EDC96) began in 1996–1997 and it reached a depth of 788 m, spanning about 45 kyr. A new drilling (EDC99) was started a few meters from EDC96 during the 1999–2000 campaign and it reached the depth of 3200 m. In this paper we discuss stratigraphic data from the EDC96 ice core but we refer also to a dust event recorded in EDC99.

[7] EDC96 dating (EDC1 timescale) was obtained by an ice-flow model based on a constant horizontal strain rate of the upper part of the ice sheet, a shear layer below with horizontal strain rate decreasing linearly with depth [e.g., Dansgaard and Johnsen, 1969], and a basal sliding velocity proportional to the horizontal surface velocity. The vertical strain is readily derived by observing continuity. See Schwander *et al.* [2001] for further information.

[8] High-resolution sulphate (1 measurement about every 4 cm) and ECM (1 cm averaged data) profiles were obtained in the field by methods described elsewhere [Udisti *et al.*, 2000; Wolff *et al.*, 1999]. ECM has to be performed on “fresh” ice (especially for firn). Since ECM equipment was not available during the first EDC96 drilling season (100-m casing), ECM measurements of the uppermost 100 m were carried out on a firn core (named Firetracc) drilled about

300 m from the main hole during the 1998–1999 season. A constant depth offset (about 90 cm) between Firetracc and EDC96 ice cores, probably due to a wrong surface reference estimation, was found by volcanic signatures comparison and therefore corrected [Udisti *et al.*, 2000].

[9] Vostok ice core chemical data were obtained at 25 m intervals [Legrand *et al.*, 1988] so we used ECM data for a detailed comparison with EDC96. The Vostok ECM record was measured on three adjacent ice cores (named BH8, BH7 and 5G), covering different depth intervals with overlapping ends, stratigraphically correlated by major volcanic signatures. BH8 covers from the surface to 130 m depth, BH7 from 130 m to 236 m and 5G is used between 236 m to the bottom. The offset depth between BH7 and BH8 is only a few cm and was neglected, whereas there is an offset of 3.34 m between BH7 and 5G. The GT4 chronology [Petit *et al.*, 1999] was developed for a fourth Vostok ice core (named 4G) that is close to 5G, and therefore adopted for the 5G core without offset. GT4 timescale was obtained by an ice-flow model similar to that used for EDC96 dating but taking into account that: (1) the ice below Vostok follows a flow line originating from Ridge B (unlike Dome C, Vostok is not located on a Dome) and (2) subglacial Lake Vostok affects layer thinning by melting and basal sliding at the bottom of the ice sheet. See Petit *et al.* [1999] for further information.

[10] Continuous isotopic measurements are available at both sites. The δD record [Jouzel *et al.*, 1987, 2001] is used as the proxy of temperature change and the $\delta^{18}O$ record [Vimeux *et al.*, 2001; Stenni *et al.*, 2001] allows the extraction of additional information from the deuterium-excess record ($d = \delta D - 8 * \delta^{18}O$). The typical resolution was 55 cm for EDC96 (corresponding to about 20, 35 and 45 years during the Holocene, transition and Last Glacial Maximum-LGM, respectively) and from 50 cm to 1 m for the Vostok ice core. 1 m depth resolution represents a temporal resolution of about 50, 75 and 90 years, in the three time periods.

3. Matching

[11] Figure 2 shows δD , ECM and sulphate profiles for the EDC96 core and δD and ECM profiles for the Vostok core. The profiles, which cover the last 45 kyr, were plotted using their original age scales: EDC1 [Schwander *et al.*, 2001] for EDC96 and GT4 [Petit *et al.*, 1999] for Vostok.

[12] The isotopic profiles (Figures 2a and 2b), used as the proxy for local temperature changes, show a similar pattern for the two sites during the Holocene and the last glacial-interglacial transition but significant variations are observed in the older ice. Both the EDC96 and Vostok timescales were estimated using a glaciological model fitted to particular events, such as the end of the Younger Dryas (taken at about 11.5 kyr BP) and the end of the ACR (circa 12.7 kyr BP), as common temporal horizons. This gives coherency for the two age scales and isotope records over the last 15 kyr. However, for deeper ice, the isotopic records are clearly shifted. In particular, a warm event dated around 38 kyr BP in EDC96 (A1 Blunier and Brook [2001]), is recorded at circa 35 kyr BP in the Vostok ice core. This was already noted by Schwander *et al.* [2001] since a ^{10}Be event occurs at 38 kyr BP on Vostok but was assigned to 41 kyr BP on EDC1.

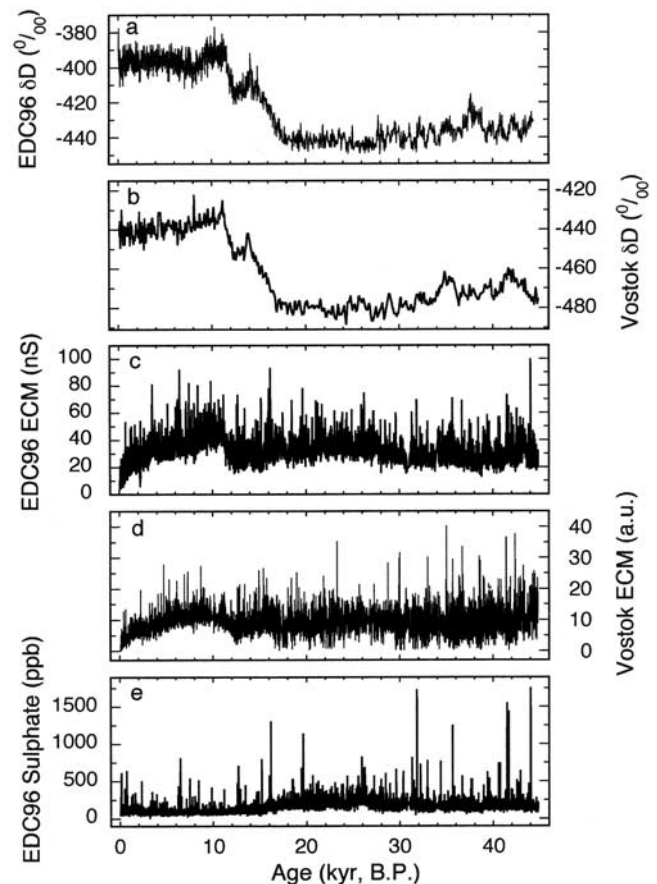


Figure 2. Records of (a and b) δD , (c and d) ECM, and (e) sulphate for EDC96 and Vostok ice cores. Data are plotted versus their original glaciological timescales. Isotopic records (δD) are from Jouzel *et al.* [2001] and Stenni *et al.* [2001] for EDC96 and from Petit *et al.* [1999] for Vostok. Although the isotope profiles display a similar pattern, a 3-kyr offset is observed between the two records. ECM is in nS for EDC96 (and Firetracc) and in arbitrary units (AU) for Vostok (BH8, BH7 and 5G ECM profiles were calibrated between them but a calibration in nS was not performed).

[13] ECM peaks (Figures 2c and 2d) are mainly related to volcanic depositions of sulphuric acid, as shown by the sulphate profile (Figure 2e); several of these events are recorded in both ice cores and were used as stratigraphic markers. Figures 3–5 show three examples of the fit among volcanic signatures in electrical (Figures 3a, 3b, 4a, 4b, 5a, and 5b) and sulphate profiles (Figures 3c, 4c, and 5c) of three EDC96 and Vostok ice core sections: the last millennium (6–45 m, 25–860 years BP; Figure 3), the late transition-early Holocene period (260–400 m, 8.1–13.2 kyr BP; Figure 4) and a section covering part of the glacial period (430–570 m, 14.7–27.3 kyr BP; Figure 5); depths and ages are expressed as EDC96 values.

[14] Figure 3 shows several known and well-dated volcanic events. Some examples include the double spikes associated with the eruption of Tambora (1815 A.D.) and an unknown eruption 5–6 years earlier (12–13 m on EDC96); the Kuwae eruption (1452 A.D. –29.8 m on EDC96); the

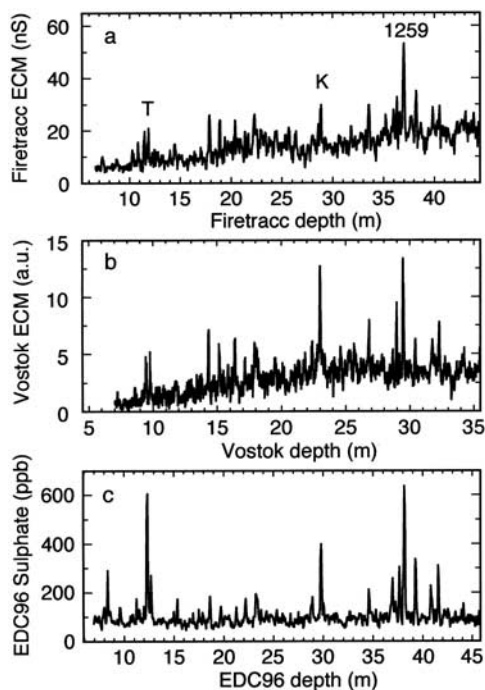


Figure 3. Peak-to-peak volcanic comparison between EDC96 and Vostok ice cores for the last millennium. The depth is expressed as real depth. ECM is in nS for Firetracc and in arbitrary units (AU) for Vostok (BH8, BH7, and 5G ECM profiles were calibrated between them, but a calibration in nS was not performed). Tambora (T), Kuwae (K), and “1259 sequence” events are also shown.

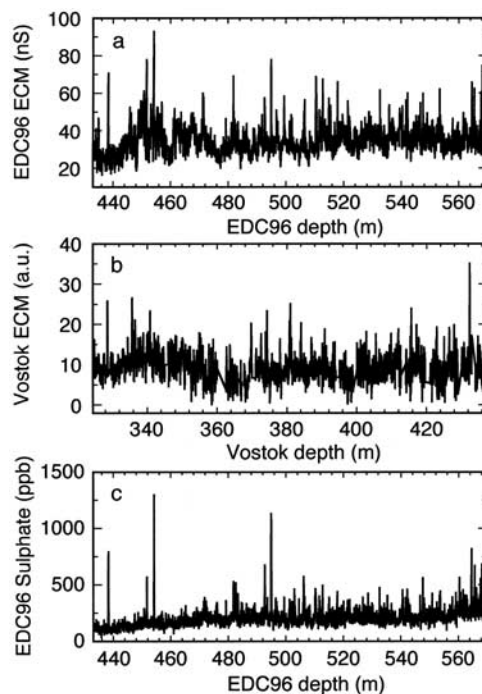


Figure 5. Peak-to-peak volcanic comparison between EDC96 and Vostok ice cores for the last part of the glacial period (about 14.7–26.4 kyr BP). The depth is expressed as real depth. ECM is in nS for EDC96 and in arbitrary units (AU) for Vostok (BH8, BH7, and 5G ECM profiles were calibrated between them, but a calibration in nS was not performed).

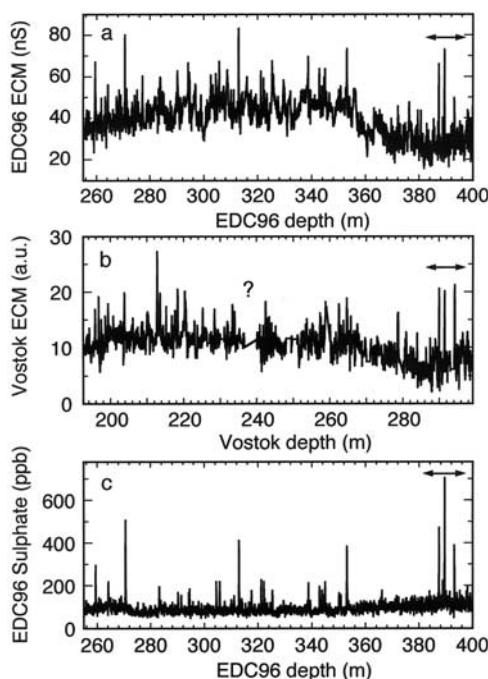


Figure 4. Peak-to-peak volcanic comparison between EDC96 and Vostok ice cores for the glacial/interglacial transition (about 8–13.2 kyr BP). The depth is expressed as real depth. ECM is in nS for EDC96 and in arbitrary units (AU) for Vostok (BH8, BH7, and 5G ECM profiles were calibrated between them, but a calibration in nS was not performed).

four peak series known as the “1259 sequence,” recorded in the 37–40 m depth interval. These events are the most used temporal horizons both in Greenland and Antarctic ice cores because of their global impact (e.g., *Langway et al.* [1995]; see also *Udisti et al.* [2000] for characterization of these events in the EDC96 ice core).

[15] Figure 4 shows a section that covers the second part of the isotopic glacial-interglacial transition and the early Holocene. The acidic transition (as revealed by ECM background increase due to lower buffer concentrations; Figures 4a and 4b) between glacial and less-dusty interglacial conditions (from 380 to 340 m depth on EDC96) is recorded in the two ice cores. An unusual triplet of volcanic events, around 390 m in EDC96, corresponds to a signal in the Vostok core with similarity both in shape and in intensity (horizontal bar in Figures 4a–4c). The matching between the two records is not perfect and some events are present only in one record but absent in the other. For example, a significant event at 314 m depth on EDC96 (Figures 4a and 4c) is not recorded in Vostok, probably because of the poor quality of the corresponding ice core section (marked with “?” in Figure 4b).

[16] Figure 5 displays a depth interval for the last part of the glacial period and the early isotopic transition. The background ECM signal is lower, likely because of a lower total acidic content, making the ECM record noisier (Figures 5a and 5b). Likewise, neutralizing effects by aerosol components can decrease the intensity of ECM volcanic signatures. Conversely, the height of volcanic

sulphate spikes is not dependent on acidity. Indeed, two very large events ($\text{SO}_4^{2-} > 1$ ppm) are observed at 454 and 496 m on EDC96 (Figure 5c).

[17] The matching of the two volcanic sequences is straightforward for the Holocene (0–360 m), where a large number of common events was easily recognized. Back in time, synchronization during the transition (11.5–18 kyr) is made easy by the δD and ECM trends and by some peculiar volcanic sequences (e.g., the triplet at 390 m depth). In the late glacial (18–45 kyr) the comparison was more difficult because of the higher ECM noise and the different relative heights shown by volcanic sequences recorded in the two ice cores. On the other hand, differences in volcanic fluxes of the same event recorded in different Antarctic sites are a common feature, due to the variability of the atmospheric fallout [e.g., *Cole-Dai et al.*, 1997]. A reliable synchronization was obtained identifying few unambiguous common volcanic events (e.g., volcanic signatures n. 33, 36, 37, 43, 46, 56 and the triplet 50–52, in Table 1) and by using some significant events (such as ^{10}Be peak, A1 interstadial maximum, a peculiar dust peak, see section 4) as temporal markers. A more detailed fit was successively carried out by stretching the Vostok depth scale to fit the other volcanic peaks in the depth intervals between the main signatures.

4. Depth-to-Depth Relationship

[18] Following the procedure described above, a total of 145 common volcanic events, recorded as sulphate (126) or ECM (19) spikes in EDC96, was recovered. Major common events are listed in Table 1.

[19] To reliably compare the ice core depths recording the same volcanic events, it is necessary to correct them for layer thinning. This effect is due to the strain within the glacier that is driven by vertical and horizontal forces arising from accumulation-rate and ice-flow processes. Such correction is accomplished with regional glaciological models that incorporate parameters related to the drilling site (bedrock topography, ice flow, surface slope, accumulation rate) to establish the initial chronology for each ice core. Model output leads to a thinning function for the EDC1 and GT4 chronology that is used to estimate the original ice-layer thickness.

[20] Figure 6 shows the relationship between the thinning-corrected ice-equivalent depths of the common events recorded in EDC96 and Vostok ice cores. Three regression lines are calculated: a general polynomial regression (PR) using the whole data set, and two linear regressions (LR1 and LR2) for the first ~ 500 m (corresponding to ~ 20 kyr) and from 500 m to bottom (from ~ 20 to 45 kyr) encompassing the glacial period:

$$\text{PR : VK} = 2.40 + 1.26 \text{ DC} + 1.35 \cdot 10^{-3} \text{ DC}^2 - 3.03 \cdot 10^{-6} \text{ DC}^3 + 1.67 \cdot 10^{-9} \text{ DC}^4 \quad (\text{R} = 0.9999) \quad (1)$$

$$\text{LR1 : VK} = -2.39 + 1.44 \text{ DC} \quad (\text{R} = 0.9999) \quad (2)$$

$$\text{LR2 : VK} = 130.2 + 1.12 \text{ DC} \quad (\text{R} = 0.9990). \quad (3)$$

Table 1. Depth and Age of the 56 Major Common Volcanic Events for EPICA Dome C and Vostok Ice Cores^a

Progressive Number	Real Depth, m		Unthinning IE Depth, m		Age, years BP		Age Offset, years
	EDC96	Vostok	EDC96	Vostok	EDC96	Vostok	
1	11.23	8.55	4.54	3.42	110	128	-18
2	12.34	9.43	5.07	3.77	130	147	-17
3	12.68	9.76	5.24	3.91	136	153	-17
4	15.36	11.86	6.59	4.85	186	201	-15
5	29.77	23.00	14.79	10.41	497	474	23
6	34.55	26.82	17.80	12.52	609	586	23
7	36.96	28.67	19.38	13.62	667	640	27
8	38.12	29.47	20.15	14.10	695	663	32
9	39.22	30.42	20.89	14.67	722	693	29
10	40.79	31.74	21.93	15.46	761	735	26
11	41.52	32.28	22.44	15.82	779	753	26
12	64.20	49.89	39.18	27.89	1349	1353	-4
13	74.88	57.96	47.84	34.07	1648	1658	-10
14	97.12	75.09	67.28	48.16	2334	2357	-23
15	125.33	96.62	93.99	67.43	3258	3312	-54
16	133.84	102.83	102.46	73.26	3548	3595	-47
17	144.93	111.39	113.67	81.42	3925	3985	-60
18	169.44	129.85	138.91	99.53	4792	4846	-54
19	176.14	134.83	145.88	104.49	5031	5088	-57
20	208.75	159.10	180.24	128.87	6205	6242	-37
21	209.89	159.93	181.46	129.72	6247	6282	-35
22	215.94	164.25	187.89	134.12	6473	6494	-21
23	232.75	176.64	205.86	146.65	7111	7111	0
24	243.33	184.23	217.24	154.40	7488	7487	1
25	251.40	189.98	225.96	160.27	7759	7765	-6
26	259.44	195.81	234.68	166.23	8044	8057	-13
27	270.59	203.83	246.81	174.43	8440	8445	-5
28	350.08	262.45	335.04	234.52	11062	11126	-64
29	387.44	289.94	377.55	262.77	12607	12650	-43
30	389.45	291.41	379.85	264.28	12710	12740	-30
31	393.15	294.21	384.11	267.16	12898	12907	-9
32	404.30	302.92	396.97	276.14	13457	13431	26
33	438.30	328.62	436.63	302.67	15199	14968	231
34	454.19	340.83	455.37	315.32	16197	15793	404
35	471.49	354.85	475.92	329.89	17541	16837	704
36	492.75	372.65	501.39	348.47	19458	18296	1162
37	494.85	374.29	503.92	350.19	19647	18430	1217
38	506.21	384.03	517.64	360.42	20672	19244	1428
39	510.27	386.98	522.56	363.52	21034	19483	1551
40	515.00	390.77	528.30	367.52	21460	19808	1652
41	532.55	402.68	549.72	380.11	23041	20793	2248
42	540.59	409.77	559.59	387.64	23750	21383	2367
43	564.62	432.36	589.30	411.79	25915	23316	2599
44	599.02	460.48	632.41	442.23	28922	25695	3227
45	616.30	479.49	654.33	463.04	30360	27297	3063
46	632.70	496.49	675.30	481.81	31829	28766	3063
47	646.35	511.15	692.88	498.12	33002	30009	2993
48	666.82	535.16	719.45	525.07	34757	32029	2728
49	677.66	547.33	733.63	538.85	35643	33027	2616
50	701.12	571.76	764.57	566.75	37582	34975	2607
51	701.72	572.39	765.37	567.47	37627	35022	2605
52	703.07	573.75	767.16	569.03	37727	35126	2601
53	724.42	594.08	795.66	592.49	39379	36714	2665
54	726.87	596.45	798.95	595.24	39597	36901	2696
55	750.97	617.75	831.52	620.06	41675	38641	3034
56	778.36	652.77	869.02	661.37	44034	41432	2602

^aThe logging depth has been converted to ice equivalent (IE) depth to take into account the firn part of the ice core. Thinning correction was calculated from the glaciological models used for EDC96 [*Schwander et al.*, 2001] and Vostok [*Petit et al.*, 1999] ice core dating. Volcanic signatures are recorded in EDC96 and Firetracc cores at Dome C and in BH8, BH7 and 5G cores at Vostok. See section 2 for information on the depth ranges covered by the different ice cores.

[21] The comparison between the transition and glacial sections was driven by using common features of the stable isotope profiles and several checkpoints (the end of the ACR, a ^{10}Be peak and a dust signal, also shown in Figure 6).

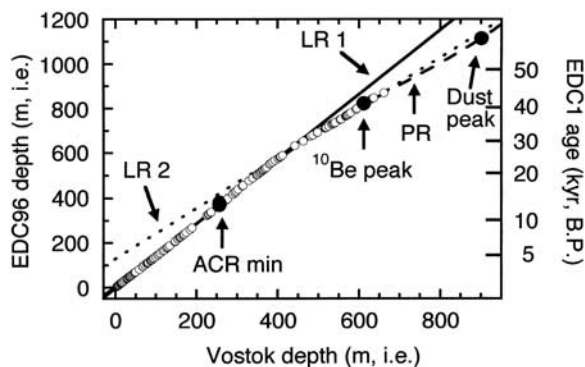


Figure 6. Depth-to-depth correlation between common volcanic signatures (145 events) recorded in EDC96 and Vostok ice cores. PR, polynomial regression (all data); LR1, linear regression for the first ~ 500 m (~ 20 kyr); and LR2, linear regression for the deeper core (20–45 kyr). Antarctic cold reversal (ACR) minimum (around 12.7 kyr BP, 290 m depth at Vostok and 390 m at Dome C); ^{10}Be event (41 kyr BP, 610 m depth at Vostok and 740 m depth at Dome C) and dust event (57.2 kyr BP, 849 m at Vostok and 947 m at Dome C-EDC99 ice core) are shown.

The ACR is a cold event occurring during the climatic transition and its minimum was found at about 390 m depth in EDC96 and about 290 m depth in Vostok. A ^{10}Be event likely associated to the Laschamp geomagnetic excursion at about 41 kyr BP is found at ~ 740 m depth on EDC96 (G. M. Raisbeck, personal communication, 2003) and ~ 610 m at Vostok [Yiou *et al.*, 1985]. The use of a dust event as checkpoint comes from the comparison between the profile of the total dust concentration from the new deeper EPICA ice core (EDC99) and the Vostok record (B. Delmonte, unpublished data, 2003). This event is found at about 950 m in EDC99 and about 850 m at Vostok and corresponds to the end of a cold stage (marine isotopic stage 4).

[22] The depth-to-depth correlation (Figure 6) clearly shows a gradual change in the ratio between snow accumulation rates (expressed by the inflection of the polynomial regression line) as the depth increases. During the last 20 kyr (including Holocene), the Dome C-Vostok accumu-

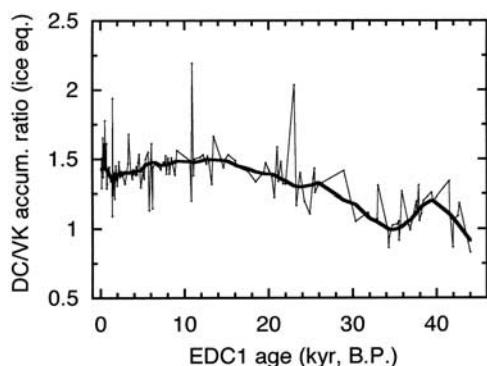


Figure 7. EDC96 to Vostok accumulation ratio as deduced from ratios of thinning-corrected ice-equivalent depths (from Table 1); the bold line shows an experimental data smoothing (running 10% weighted fit).

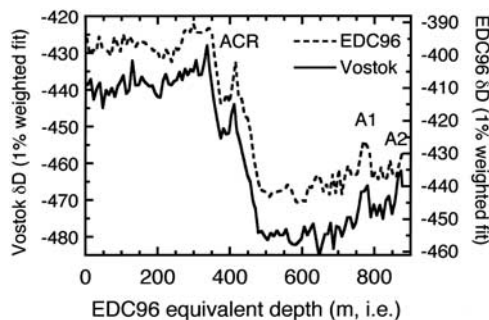


Figure 8. EDC96 and Vostok isotope profiles plotted on a common depth scale (EDC96) after the stratigraphic synchronization. Vostok depths have been converted to equivalent EDC96 depth using equation (1) (polynomial regression). Smoothing of δD profiles was obtained by a running 1% weighted fit.

lation ratio is 1.44 (slope of LR1) while this ratio decreases to 1.12 (slope of LR2) for the transition and the glacial period reaching the minimum value (1.0) at 35 kyr BP (Figure 7), showing that the two sites experienced the same accumulation rates in this period.

[23] The good fit between stratigraphic markers gives confidence to our matching. Figure 8 shows the EDC96 and Vostok δD smoothed profiles plotted versus a common (EDC96) depth scale. The two records are consistent and the initial depth offset is now corrected as shown by the phasing of the ACR oscillation and the A1 and A2 interstadials [Blunier and Brook, 2001] at the ice core bottom. A residual offset (around 10 m, roughly corresponding to 750 years) remains around 600 m, where volcanic matching was affected by several breaks in the Vostok ice core.

5. Discussion

[24] The δD comparison and the consistency with the checkpoints give confidence in our peak-to-peak fitting. The difference in the EDC1-GT4 age scales (“age offset” in Table 1) is very close to zero in the Holocene and shows the greatest differences (around 3.0–3.5 kyr) in the earlier LGM (around 30 kyr BP), remaining quite stable (around 3.0 kyr) in the rest of the glacial period. The age offset in the glacial period has to be treated carefully because it is poorly documented by a small number of reliable common events. On the other hand, the experimental data give a result very similar to the Schwander *et al.* [2001] estimation made by comparing age models, making the two approaches consistent with one another.

[25] Our data show changes in relative accumulation ratio between EPICA Dome C and Vostok. A lower Dome C-Vostok ratio (Figure 7) during the glacial period could be interpreted as an accumulation rate decrease greater than expected at Dome C, or lower than expected at Vostok, or a combination of both. This behavior is somewhat unexpected because we expect glacial accumulation-rate values to be lower than Holocene values in a similar way at both sites. Why then does EPICA Dome C undergo larger changes (Holocene/LGM accumulation ratio ~ 2) with respect to Vostok (Holocene/LGM accumulation ratio ~ 1.5)? Although snow accumulation rates in central East Antarctica are very small, the change in relative accumulation rate that

we observe here is highly significant and persistent, and well beyond any of the potential errors. Indeed, the change in the ratio of the accumulation is about 40% between glacial and Holocene conditions; this means an absolute change of about $0.7 \text{ g cm}^{-2} \text{ a}^{-1}$ at Vostok (present-day accumulation rate = $2.2 \text{ g cm}^{-2} \text{ a}^{-1}$) and about $1.2 \text{ g cm}^{-2} \text{ a}^{-1}$ at Dome C (present-day accumulation rate = $2.7 \text{ g cm}^{-2} \text{ a}^{-1}$), considering a glacial accumulation rate of about $1.5 \text{ g cm}^{-2} \text{ a}^{-1}$ in both stations. Such a difference becomes significant when it is integrated over thousands years, between the volcanic markers.

[26] It is important to note that all the accumulation ratios were measured by depth differences between pairs of synchronous volcanic horizons recorded in both EDC96 and Vostok ice cores. Depth differences calculated in this way yield accumulation-rate ratios that are independent of dating models, except for thinning calculations, and of accumulation-rate values deduced from δD profiles. The uncertainties associated to the thinning-correction procedure are not easy to evaluate, but a good estimation can be obtained by the dating uncertainty. Indeed, EDC1 and GT4 timescales were obtained by coupling a thinning function (from an ice-flow model) with the accumulation rate (coming from δD profiles); therefore, the dating errors could be considered as the cumulative uncertainties on the two factors. In particular, for EDC1, *Schwander et al.* [2001] estimate uncertainties of 10, 200 and 2000 years in the last 700, 10,000 and 41,000 years, respectively. These values correspond to depth uncertainties (after thinning correction) lower than 5%, also in the glacial period, where the ice layer thinning is relevant. EDC1 and GT4 timescales show that accumulation rates in the interglacial period are 100% and 50% higher than in the glacial period at Dome C and Vostok, respectively; therefore, we can assume that such variations are significant with respect to the thinning-correction and accumulation-rate uncertainties. This is reasonably true also for the Dome C-Vostok accumulation ratio, showing an increase of 40% from glacial to interglacial conditions (Figure 7). When a peak-to-peak procedure to evaluate accumulation rates was applied to uncorrected data (thinned real ice depths), the EDC96/Vostok accumulation ratio gives 1.37 in the Holocene and 0.99 in the glacial period; these values are only slightly lower than reported above (1.44 and 1.12, respectively), confirming that the procedure accounting for thinning can be considered negligible. The relative trend in snow accumulation at Dome C and Vostok could be ascribed to several factors such as glaciological and/or climatic effects, including atmospheric-transport changes that we discuss in the next sections.

5.1. Changes in Thickness of the Ice Sheet

[27] Unlike West Antarctica, which experienced very different geometric conditions in the LGM with respect to the Holocene and a northward shift in the grounding lines of major ice shelves (Ross and Ronne-Filchner) [*Conway et al.*, 1999; *Ritz et al.*, 2001], model simulations [*Ritz et al.*, 2001] suggest that the East Antarctic ice sheet was more stable, its evolution being mainly driven by accumulation-rate variability. In the model of the Antarctic ice sheet evolution for the last 420 kyr proposed by *Ritz et al.* [2001], ice shelf extension in the Pacific/Indian Sector did not vary greatly during the LGM, and the decrease in the

elevation of East Antarctica was estimated to be about 100 m in the Vostok region. These variations may have changed the seaward flow of ice, but to a lesser extent than in West Antarctica. Both Dome C and Vostok were probably affected by the same geometric changes due to their relative proximity and similar elevation. For these reasons, we speculate that the two sites experienced similar changes in elevation and ice flow, and that ice-flow conditions did not vary significantly.

5.2. Spatial Variation of Accumulation

[28] Vostok is located on a flow line that originates from Ridge B (300 km inland) where the present-day accumulation rate is about $3.2 \text{ g cm}^{-2} \text{ a}^{-1}$ [*Ritz*, 1992; *Siegert*, 2003], or about 1.5 times higher than Vostok ($2.2 \text{ g cm}^{-2} \text{ a}^{-1}$). In the Vostok core, ice layers at 600 m depth (about 40 kyr old) were deposited about 30 km upstream [*Petit et al.*, 1999; *Ritz*, 1992]. Assuming a constant linear trend in space and time along the flow line, an accumulation rate higher by about 10% of the difference between Ridge B and Vostok accumulation rate is expected, which roughly implies a 5% change in Vostok accumulation rate. Recent accumulation-rate estimates along the Ridge B-to-Vostok transect were calculated by *Siegert* [2003], on the basis of isochronous horizons in radar profiles. Unfortunately, the youngest isochronous horizon is dated 46 kyr, so that the Holocene accumulation-rate values were only estimated by a simple model and cannot be used for a comparison with our data. By using the 46-kyr isochrone, *Siegert* [2003] plots the changes in accumulation rate along the Ridge B-Vostok transect during Holocene and late glacial period. Even if the accumulation-rate remains close to $2.2 \text{ g cm}^{-2} \text{ a}^{-1}$ along the transect, some relevant changes can be observed, with a maximum value (around $2.7 \text{ g cm}^{-2} \text{ a}^{-1}$) near Ridge B and a minimum value (around $1.8 \text{ g cm}^{-2} \text{ a}^{-1}$) about 130 km from Vostok. We roughly evaluated the cumulative accumulation-rate change in the 30-km transect upstream of Vostok by integrating the accumulation rate profile (46–0 kyr isochrones *Siegert* [2003, Figure 5]) and obtained an accumulation rate at Vostok that is about 10% higher. This relative variation is higher than that estimated above from the present time accumulation rates at Vostok and Ridge B (about 5%), but it is significantly lower than the observed changes. Indeed, our data imply that the Dome C-Vostok accumulation ratio changes from 1.44 in the Holocene to a minimum of 1.0 at 35 kyr (Figure 7), with a variation of about 44%. Therefore the change in the deposition site through time can account for only a minor part of the changes in Dome C-Vostok accumulation ratios from the glacial period to the Holocene. We also note that for the Dome C area, geographical variations of accumulation are also present as shown by an accumulation rate at the EPICA site 10% lower ($2.7 \text{ g cm}^{-2} \text{ a}^{-1}$) than that found at the old Dome C site ($3.1 \text{ g cm}^{-2} \text{ a}^{-1}$) located 55 km away [*Petit et al.*, 1982].

5.3. Accumulation Rate Deduced From Modeling

[29] In the absence of seasonal stratigraphies and absolute chronological markers, ice core accumulation rate is estimated by glaciological models. The key assumption of glaciological models is the dependence of accumulation rate on water vapor pressure and therefore on the local temper-

ature. Accumulation changes are taken as the derivative of the saturation pressure with respect to the temperature at the level where the precipitation forms, i.e., above the inversion layer. This relationship is based on a simple 1-D transport model assuming a constant (through time) airflow to the site and therefore no significant change in the atmospheric circulation [Ritz, 1992]. The temperature is inferred directly from the ice core isotopic profiles. In a conventional approach, temperature change is estimated assuming a temporal isotope-temperature slope (at a given site through time) equals the present-day spatial slope. During the last glacial period, surface temperature was $\sim 10^{\circ}\text{C}$ lower than present and $\sim 6^{\circ}\text{C}$ lower at the inversion level, leading to a lower vapor content and to an estimated snow accumulation rate about 50% lower than the present-day.

[30] By using these assumptions for both EDC96 and Vostok cores, a similar change in temperature would yield an almost constant accumulation ratio (i.e., close to 1.4), but this is not supported by our observations. Jouzel *et al.* [2003] review the various arguments underlying the use of the present-day spatial slope to interpret the ice core δD and $\delta^{18}\text{O}$ profiles from the East Antarctic Plateau and conclude that the present-day spatial slope appears to be the best surrogate, within -10% to $+30\%$ accuracy, of the temporal slope. In this way, as the glacial-to-interglacial isotopic changes at Vostok and EPICA Dome C are of the same magnitude (Figure 8), we expected similar changes in accumulation rate. The change in the Dome C-Vostok ratio, as we observed, would imply a glacial to Holocene temperature change lower by 20% (or higher by 20%) at Vostok (or at Dome C). Since the Vostok area experiences deep continental conditions, with a surface temperature lower than Dome C (-55°C and -53.5°C respectively), a lower accumulation rate (among the lowest from Antarctic sites), as well as the highest depleted isotope content of snow, Vostok temperatures were probably continuously lower than for Dome C also during the glacial period. These arguments suggest that a change in the relative temperatures of the two sites cannot be used to explain the observed relative accumulation variation.

[31] In summary, neither glaciological effects nor our temperature interpretation of the isotopic records can explain the observations. An alternative explanation is that accumulation change depends not only on temperature (thermodynamic effect) but is influenced by modification in atmospheric circulation processes.

5.4. Regional Variation of the Atmospheric Circulation

[32] Changes in moisture sources and in atmospheric transport processes may drive variability of accumulation. Actually, there is only limited evidence from stable isotopes (δD) to account for differences in accumulation processes, since δD variations for the glacial period at Dome C and Vostok (Figure 8) are very similar. Vimeux *et al.* [1999, 2001] used the deuterium excess as a proxy for past temperatures of the ocean source of moisture for Vostok. For the glacial period it was suggested that the source was located at lower latitudes, with respect to the Holocene, and that a higher meridional transport prevailed. On the other hand, by observing the variations in the deuterium-excess profile calculated at Dome C, Stenni *et al.* [2001] supported

the idea that the ocean sources supplying moisture to Vostok and Dome C could be different, at least in the Holocene. We postulate that transport pathways carrying humid air masses from the ocean areas to Vostok and Dome C were so different in the glacial period to justify a significant change in the accumulation ratio at the two sites.

[33] General circulation models (GCM) indicate a scenario for glacial time characterized by a larger poleward thermal gradient and a more intense and persistent polar vortex than for interglacial period simulations [Krinner and Genthon, 1998]. In the glacial period, a persistent vortex and pronounced thermal anticyclone may have acted as a barrier to the intrusion of midlatitude air masses. Lunt and Valdes [2001], using back-trajectories around Antarctica to Dome C for LGM and at present-day calculated by re-analyses and simulations, suggested that the polar vortex forces the air masses to cover longer trajectories around Antarctica.

[34] In addition to this general pattern, there is increasing evidence of variable transport of the aeolian continental dust toward Antarctica between the glacial period and the Holocene as well as evidence for variability in transport from site to site (B. Delmonte, unpublished data, 2003). The Antarctic glacial atmosphere was dusty as supported by considerable evidence from all Antarctic ice records, due to a drier atmosphere, increased continental aridity and a probable faster atmospheric transport [e.g., see Petit *et al.*, 1999, and references therein]. The dust size distribution is a relevant proxy of the transport pathway in which coarser particles are associated to a more rapid transfer and finer particles to a longer pathway [Ruth *et al.*, 2003]. At Vostok, de Angelis *et al.* [1984] observed coarser particle sizes during the glacial period with respect to the Holocene. On the contrary, for EPICA Dome C, glacial dust appears more graded than the Holocene dust [Delmonte *et al.*, 2002], which is attributed to greater difficulties for midlatitude air masses to penetrate the isolated Antarctic continent and to reach the site. Such regional variability in the dust transport to different sites in East Antarctica is supported by additional dust analyses performed on the Dome B and Komsomolskaya ice cores, both covering the last deglaciation (B. Delmonte, unpublished data, 2003). These regional differences in atmospheric transport suggested by the dust data may indicate changes in moisture advection and therefore accumulation-rate changes in East Antarctica.

[35] When the thermal anticyclone over Antarctica is stable and the cold air of the low troposphere is pushed out by the katabatic winds, an advection of air toward central areas has to occur at the upper levels of the atmosphere (typically higher than 4–5 km altitude). For example, currently during the austral winter heat and moisture is advected inland making the so-called “coreless winter” [Schwerdtfeger, 1984]. Strengthening of the anticyclone may lead to air advection from different altitudes and the level of the advection likely depends on the synoptic situation, regional orography, the location of cyclonic areas around Antarctica, and sea-ice extent. As moisture generally decreases with altitude, we can attribute a negative anomaly in accumulation rate at the site to the advection of air from higher altitude. In the same way, if we assume that the continental particle grade is linked to altitude, we can suppose that the smaller particles would imply higher-altitude transport pathways.

[36] The observed shift toward lower size of the glacial-age particles at Dome C, with respect to the Holocene, supports the idea that the Dome C region could have been affected mainly by high-altitude air-mass transport in the cold period, causing negative anomalies in the accumulation rate. Indeed, our data support this view, revealing a glacial accumulation rate lower than expected, so that the Dome C-Vostok ratio drops to values near to 1.0 from the higher Holocene values. On the other hand, the same effect could have been caused by positive accumulation anomalies at Vostok, if the rapid advection of lower-altitude, wetter air masses, potentially demonstrated by coarser dust-particle size, affected this area under the influence of a more efficient meridional transport. Our postulated mechanism of atmospheric-circulation changes at regional scales during the glacial period needs to be checked and modeled in GCM experiments.

6. Conclusions and Implications for Ice Core Dating Strategy

[37] A stratigraphic link between EDC96 and Vostok ice cores was made using volcanic markers, enabling the estimation of relative changes in snow accumulation rates at the two sites. The EPICA Dome C-Vostok accumulation ratio is close to 1.0 at 35 kyr BP and increases during the climatic transition reaching a near-constant value of about 1.4 in the Holocene. With respect to the accumulation rate as estimated from the conventional approach based on temperature (deduced from the stable-isotope content), the low glacial ratio is understood either as a negative anomaly in accumulation rate at Dome C or positive anomaly at Vostok or simultaneous changes in both accumulations.

[38] Glaciological effects, layer thinning models and the variability in δD or deuterium excess are unable to account significantly for the ratio changes. More likely, variations in regional atmospheric circulation, as suggested by changes of the dust-size distribution, appear to be an encouraging explanation. Strengthening of the thermal anticyclone during the glacial period may have led to advection of air from a different altitude. Superimposed on a general trend of cooling and lower accumulation rates at both sites during the glacial period, a negative anomaly in accumulation rate at Dome C may be associated with advection of air from higher levels. In contrast, a positive anomaly at Vostok may be associated with advection of air from lower levels. Interestingly, a combination of these scenarios appears consistent with the different gradation of dust particles and with the deuterium excess pattern.

[39] Our results raise an important issue in the assessment of dating strategies for future ice cores in Antarctica. The assumption of accumulation rate depending only on temperature change, as derived from the conventional approach, needs modification. While the isotope-temperature temporal slope could still be very close to the modern spatial value, the existence of accumulation changes not directly linked to temperature has to be considered. Such a component could be seen only through the high-resolution stratigraphic link such as we develop here. Parrenin [2002] and Parrenin *et al.* [2001] have developed an inverse approach for dating several deep ice cores at the same time to take into account a parameter that is variable in time and space from core to

core. That approach allows for free parameters to estimate nonrelated temperature and isotopic changes (which may vary through time) and explicitly accounts for a nonthermal contribution to accumulation change.

[40] **Acknowledgments.** This work is a contribution to the “European Project for Ice Coring in Antarctica” (EPICA), a joint ESF (European Science Foundation)/EC scientific program, funded by the European Commission and by national contributions from Belgium, Denmark, France, Germany, Italy, the Netherlands, Norway, Sweden, Switzerland and the United Kingdom. This is EPICA publication 92.

References

- Blunier, T., and E. J. Brook (2001), Timing of millennial-scale climate change in Antarctica and Greenland during the last glacial period, *Science*, *291*, 109–112.
- Cole-Dai, J., and E. Mosley-Thompson (1999), The Pinatubo eruption in South Pole snow and its potential value to ice-core paleovolcanic records, *Ann. Glaciol.*, *29*, 99–105.
- Cole-Dai, J., E. Mosley-Thompson, and L. G. Thompson (1997), Annually resolved Southern Hemisphere volcanic history from two Antarctic ice cores, *J. Geophys. Res.*, *102*(D14), 16,761–16,771.
- Conway, H., B. L. Hall, G. H. Denton, A. M. Gades, and E. D. Waddington (1999), Past and future grounding-line retreat of the West Antarctic ice sheet, *Science*, *286*, 280–283.
- Dansgaard, W., and S. J. Johnsen (1969), A flow model and a time scale for the ice core from Camp Century, Greenland, *J. Glaciol.*, *8*(53), 215–223.
- Dansgaard, W., *et al.* (1993), Evidence for general instability of past climate from a 250-kyr ice-core record, *Nature*, *364*, 218–220.
- de Angelis, M., M. Legrand, J. R. Petit, N. I. Barkov, Y. S. Korotkevich, and V. M. Kotlyakov (1984), Soluble and insoluble impurities along the 950 m Vostok deep ice core (Antarctica), *J. Atmos. Chem.*, *1*, 215–239.
- Delmonte, B., J. R. Petit, and V. Maggi (2002), Glacial to Holocene implications of the new 27,000 year dust record from the EPICA Dome C (East Antarctica) ice core, *Clim. Dyn.*, *18*, 647–660.
- EPICA Dome C 2001–02 Science and Drilling Teams (2002), Extending the ice core record beyond half a million years, *Eos Trans. AGU*, *83*(45), 509, 517.
- Jouzel, J., C. Lorius, J. R. Petit, C. Genthon, N. I. Barkov, V. M. Kotlyakov, and V. M. Petrov (1987), Vostok ice core—A continuous isotope temperature record over the last climate cycle (160,000 years), *Nature*, *329*, 403–408.
- Jouzel, J., *et al.* (2001), A new 27 kyr high resolution East Antarctic climate record, *Geophys. Res. Lett.*, *28*, 3199–3202.
- Jouzel, J., F. Vimeux, N. Caillon, G. Delaygue, G. Hoffmann, V. Masson-Delmotte, and F. Parrenin (2003), Magnitude of isotope/temperature scaling for interpretation of central Antarctic ice cores, *J. Geophys. Res.*, *108*(D12), 4361, doi:10.1029/2002JD002677.
- Krinner, G., and C. Genthon (1998), GCM simulations of the Last Glacial Maximum surface climate of Greenland and Antarctica, *Clim. Dyn.*, *14*, 741–758.
- Langway, C. C. J., K. Osada, H. B. Clausen, C. U. Hammer, and H. Shoji (1995), A 10-century comparison of prominent bipolar volcanic events in ice cores, *J. Geophys. Res.*, *100*(D8), 16,241–16,247.
- Legrand, M., and P. Mayewski (1997), Glaciochemistry of polar ice cores: A review, *Rev. Geophys.*, *35*, 217–243.
- Legrand, M., C. Lorius, N. I. Barkov, and V. N. Petrov (1988), Atmospheric chemistry changes over the last climatic cycle (160,000 yr) from Antarctic ice, *Atmos. Environ.*, *22*(2), 317–331.
- Lorius, C. (2000), Past global changes and their significance for the future—Preface, *Quat. Sci. Rev.*, *19*(1–5), 1–2.
- Lunt, D. J., and P. J. Valdes (2001), Dust transport to Dome C, Antarctica, at the Last Glacial Maximum and present day, *Geophys. Res. Lett.*, *28*(2), 295–298.
- Parrenin, F. (2002), Datation glaciologique des forages profonds en Antarctique et modélisation conceptuelle du climat: Implications pour la théorie astronomique des paléoclimats, Univ. Joseph Fourier Grenoble I, Grenoble.
- Parrenin, F., J. Jouzel, C. Waelbroeck, C. Ritz, and J. M. Barnola (2001), Dating the Vostok ice core by an inverse method, *J. Geophys. Res.*, *106*(D3), 31,837–31,851.
- Petit, J. R., J. Jouzel, M. Pourchet, and L. Merlivat (1982), A detailed study of snow accumulation and stable isotope content in Dome C (Antarctica), *J. Geophys. Res.*, *87*(C6), 4301–4308.
- Petit, J. R., *et al.* (1999), Climate and atmospheric history of the past 420,000 years from the Vostok ice core, Antarctica, *Nature*, *399*, 429–436.

- Ritz, C. (1992), Un modèle thermo-mécanique d'évolution pour le bassin glaciaire antarctique Vostok-glacier Byrd: Sensibilité aux valeurs des paramètres mal connus, Univ. Joseph Fourier Grenoble I, Grenoble.
- Ritz, C., V. Rommelaere, and C. Dumas (2001), Modeling the evolution of Antarctic ice sheet over the last 420,000 years: Implications for altitude changes in the Vostok region, *J. Geophys. Res.*, *106*(D23), 31,943–31,964.
- Ruth, U., D. Wagenbach, J. P. Steffensen, and M. Bigler (2003), Continuous record of microparticle concentration and size distribution in the central Greenland NGRIP ice core during the last glacial period, *J. Geophys. Res.*, *108*(D3), 4098, doi:10.1029/2002JD002376.
- Schwander, J., J. Jouzel, C. U. Hammer, J. R. Petit, R. Udisti, and E. W. Wolff (2001), A tentative chronology for the EPICA Dome C Concordia ice record, *Geophys. Res. Lett.*, *28*(22), 4243–4246.
- Schwerdtfeger, W. (1984), *Weather and Climate of the Antarctic*, Elsevier Sci., New York.
- Siegert, M. (2003), Glacial-interglacial variations in central East Antarctic ice accumulation rates, *Quat. Sci. Rev.*, *22*, 741–750.
- Southon, J. (2002), A first step to reconciling the GRIP and GISP2 ice-core chronologies, 0–14,500 yr BP, *Quat. Res.*, *57*, 32–37.
- Stenni, B., V. Masson-Delmotte, S. Johnsen, J. Jouzel, A. Longinelli, E. Monnin, R. Röthlisberger, and E. Selmo (2001), An oceanic cold reversal during the last deglaciation, *Science*, *293*, 2074–2077.
- Taylor, K. C., C. U. Hammer, R. B. Alley, H. B. Clausen, D. Dahl-Jensen, A. J. Gow, N. S. Gundestrup, J. Kipfstuhl, J. C. Moore, and E. D. Waddington (1993), Electrical conductivity measurements from the GISP2 and GRIP Greenland ice cores, *Nature*, *366*, 549–552.
- Udisti, R., S. Becagli, E. Castellano, R. Mulvaney, J. Schwander, S. Torcini, and E. W. Wolff (2000), Holocene electrical and chemical measurements from the EPICA-Dome C ice core, *Ann. Glaciol.*, *30*, 20–26.
- Vimeux, F., V. Masson, J. Jouzel, M. Stievenard, and J. R. Petit (1999), Glacial-interglacial changes in ocean surface conditions in the Southern Hemisphere, *Nature*, *398*, 410–413.
- Vimeux, F., V. Masson, G. Delaygue, J. Jouzel, J. R. Petit, and M. Stievenard (2001), A 420,000 year deuterium excess record from East Antarctica: Information on past changes in the origin of precipitation at Vostok, *J. Geophys. Res.*, *106*, 31,863–31,873.
- Wolff, E. W., I. Basile, J. R. Petit, and J. Schwander (1999), Comparison of Holocene electrical records from Dome C and Vostok, *Ann. Glaciol.*, *29*, 89–93.
- Yiou, F., G. Raisbeck, G. Bourles, C. Lorius, and N. I. Barkov (1985), ^{10}Be in ice at Vostok, Antarctica, during the last climatic cycle, *Nature*, *316*, 616–617.

S. Becagli, E. Castellano, and R. Udisti, Department of Chemistry, University of Florence, Via della Lastruccia 3, I-50019 Florence, Italy. (udisti@unifi.it)

B. Delmonte, Department of Environmental Science, University of Milano-Bicocca, Piazza della Scienza 1, I-20126 Milan, Italy.

J. Jouzel, Laboratoire des Sciences du Climat et de l'Environnement, UMR CEA-CNRS, F-91191 Gif-sur-Yvette, France.

J. R. Petit, Laboratoire de Glaciologie et Géophysique de l'Environnement du CNRS, 54 rue Moliere, BP 96, F-38402 Saint-Martin-d'Herès Cedex, France.

J. Schwander, Physics Institute, University of Bern, CH-3012 Bern, Switzerland.

B. Stenni, Department of Geological, Environmental and Marine Sciences, University of Trieste, Via E. Weiss 2, I-34127 Trieste, Italy.

E. W. Wolff, British Antarctic Survey, Natural Environment Research Council, Madingley Road, Cambridge CB30ET, UK.